Journal of Energy and Power Engineering 15 (2021) 135-149
doi: 10.17265/1934-8975/2021.04.003

Comparative Analysis of the Methods Used for Active Power Filtering in a Grid-Connected Photovoltaic System

Alexandru Dusa[1], Petru Livinti[2], Nicolae Badea[1] and Laurentiu Luca[3]

1. "Dunarea de Jos" University of Galati, Domneasca Street, No. 47 Galati City, Romania

2. "Vasile Alecsandri" University of Bacau, Calea Marasesti Street, No. 157 Bacau City, Romania

3. Smartech Automation SRL, Galati City, Romania

Abstract: This paper presents a comparison of the results obtained from the integration of the photovoltaic system to the electrical grid through the Active Power Filter. The innovative aspect of this article consists of the elaboration of 4 models in Matlab/Simulink for 4 methods of control of the Active Power Filter introduced between the photovoltaic system and the alternating current grid and the highlighting of the performances obtained regarding the quality and quantity of electricity transferred for each control method in part. Following the analysis of the results, it was found that by using the Indirect Control (CI) method of the Active Power Filter, the best results are obtained THDu = 3.24%, THDi = 2.46% if the photovoltaic system produces a larger amount of energy than the nonlinear load, and by using the methods of control of the Active Power Filter Synchronous Reference Frame (DQ) and Instantaneous Power (PQ) the best results are obtained: THDu = 3.22%, THDi = 5.26% for the method (DQ) and THDu = 3.41%, THDi = 5.17% for the method (PQ) if the photovoltaic system produces a smaller amount of energy than the nonlinear load.

Key words: Photovoltaic system, active power filter, the power quality.

1. Introduction

Due to the recent increase in the integration of the renewable energy system in electrical grids, the security and stability of the operation of the electric power supply system is affected [1]. At the same time, the electric power quality is also influenced by nonlinear loads. These nonlinear tasks generate harmonic currents that interact with the impedance of the grid causes harmonic voltages that affect all consumers connected to the same Common Coupling Point (CCP) [2]. The integration of renewable energy in the electrical grid taking into account the electric power quality can be achieved through Active Power Filters supplied on the direct current side by renewable energy systems. These systems were studied in the paper [3-9] where the results of the injected renewable energy into the electrical grid were presented while reducing the harmonic level of voltage and current.

In this paper the results obtained by simulating in Matlab/Simulink were compared in the case of integration of a photovoltaic system in an alternating current grid through an Active Power Filter. The extraction of the maximum power from the photovoltaic panels is performed with the MPPT algorithm "Perturb and Observe". The architecture of the Active Power Filter of the inverter is structured in 3 levels. The control of the Active Power Filter introduced between the photovoltaic system and the alternating current grid is performed by the methods: Indirect Control (CI), Synchronous Reference Frame (DQ), Instantaneous power (PQ) and Positive Sequence Method (MSP).

For the 4 control methods of the Active Power Filter mentioned above, two distinct cases were analyzed for the photovoltaic system connected to the grid, namely:

Corresponding author: Alexandru Dusa, Ph.D. student, research fields: energy.

- The power of the photovoltaic system is higher than the nonlinear load and the excess energy is injected into the grid;
- The power of the photovoltaic system is less than the nonlinear load, and the energy difference is completed by the grid.

The innovative aspect of this article consists of the elaboration of 4 models in Matlab/Simulink for 4 methods of control of the Active Power Filter introduced between the photovoltaic system and the alternating current grid and highlighting the performances obtained regarding the quality and quantity of electricity transferred for each control method in part.

2. System Configuration

Fig. 1 presents the block diagram of the proposed system. This diagram allows the injection of power from the grid photovoltaic system, the supply of non-linear load from the grid and the photovoltaic system, the attenuation of harmonics and the improvement of the power factor.

2.1 Boost Converter

The boost converter allows the extraction of the maximum power from the photovoltaic panels using the P&O algorithm and the raising of the output voltage to the voltage level on the capacitor of the Active Power Filter. The block diagram of the boost converter is presented in Fig. 2. For designing this type of converter, it is necessary to know the following values [10, 11]: minimum input voltage U_{in_min} = 345.4 V, output voltage U_{out} = 750 V, intensity of the load current I_{out} = 9.25 A, switching frequency F_{sw} = 25 kHz, power P = 7,300 W, effectiveness η = 95%.

For the design of the boost converter and the determination of the duty cycle or used calculation formulas:

$$D = \left[1 - \frac{\left(U_{in\_\min} \cdot \eta\right)}{U_{out}}\right]\%$$

The output current I_{out} is calculated with the relation:

$$I_{out} = \frac{P}{U_{out}}$$

The value of the input current I_{in} is determined with the relation:

$$I_{in} = \frac{P}{U_{1n}}$$

The value of the input current I_{in} is equal to the current rate in the coil ΔI_L. The ripple current of the inductance L will be equal to 10% of the input current I_{in}:

$$\Delta I_L = I_{in} \cdot 10\%$$

The inductance L is calculated through the relation:

$$L = \frac{U_{in} \cdot D}{\Delta I_L \cdot F_{sw}}$$

The value of the ripple voltage ΔU_{out} will be equal to 1% of the value of the output voltage U_{out}:

$$\Delta U_{out} = U_{out} \cdot 1\%$$

The calculation of the output capacity is performed with the relation:

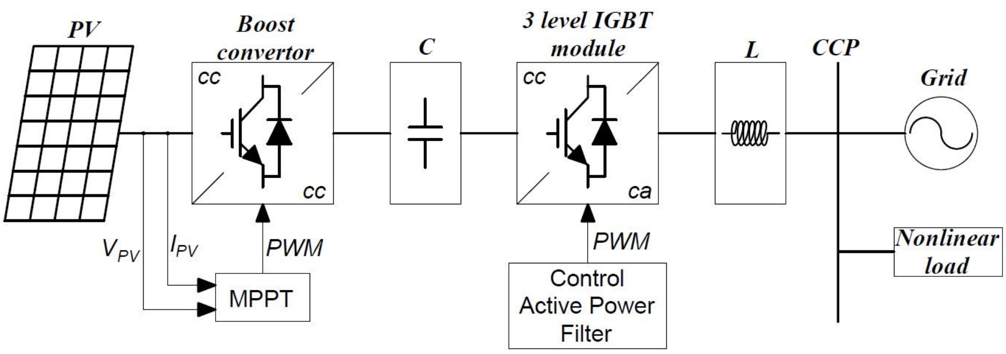

Fig. 1 Block diagram of the system.

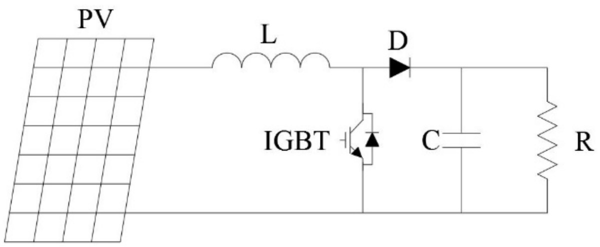

Fig. 2 Boost converter.

$$C = \frac{I_{out} \cdot D}{F_{sw} \cdot \Delta U_{out}}$$

The load resistance is calculated by the relation:

$$R = \frac{U_{out}}{I_{out}}$$

2.2 Maximum Power Point Tracking Algorithm

The extraction of the maximum power from the photovoltaic panels is done with the help of the Perturb and Observe algorithm (Fig. 3) [11, 12].

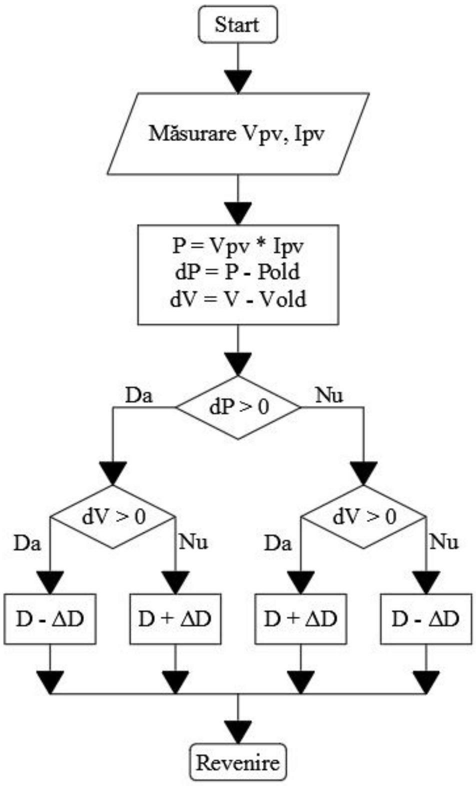

Fig. 3 Diagram of the Perturb and Observe algorithm.

This method consists of periodically changing the voltage of the photovoltaic panels and measuring the power. When the power obtained increases with the change of voltage in a certain direction, this direction is maintained at the next iteration. If the power obtained is lower than the previous value, the search direction is changed.

2.3 Active Power Filter Control

2.3.1 Indirect Control (CI)

This strategy does not require knowledge of the spectrum of electric current absorbed by the nonlinear load [11, 13].

$$i_s a(t) = i_c a(t) + i_f a(t)$$

The electric current absorbed by the nonlinear load is:

$$i_c a(t) = i_c^1 a(t) + \sum_k i_c a_k(t) + i_c a_q(t)$$

where:

$i_c^1 a(t)$ —fundamental active component of load current;

$\sum_k i_c a_k(t)$—harmonics sum of load current;

$i_c a_q(t)$—reactive component of load current.

The electric current through the Active Power Filter is:

$$i_f a(t) = i_f^1 a(t) + \tilde{i}_f a(t)$$

where:

$i_f^1 a(t)$ —fundamental active component of APF current;

$\tilde{i}_f a(t)$—harmonics sum of APF current.

The electric current absorbed by the grid must be sinusoidal and must have the same phase as the voltage. The component to be compensated by the Active Power Filter is given by:

$$\tilde{i}(t)=\tilde{i}_f a(t)+\sum_k i_c a_k(t)+i_c a_q(t)$$

From the above formulas we obtain:

$$i_{sa}=i^1_{La}+i^1_{fa}+\tilde{i}$$

The signal is generated for the charging input of the current regulator of phase a of the power supply:

$$i^*_a(t)=\varepsilon_{DC}\frac{v_a}{\sqrt{2}V}=\varepsilon_{DC}\sin\omega t$$

where: V is the effective value of the phase voltage of the grid and ε_{DC} the output of the DC voltage regulator.

The above charge is compared with the measured value of the electric current absorbed from the i_{sa} grid, resulting for the control of the Active Power Filter:

$$i_{ref}a=k\left(i^*_a-i_{sa}\right)=k\left(i^*_a-\tilde{i}-i^1_c a-i^1_f a\right)$$

where: k is the amplifier of the regulator.

The regulator is linear, the sinusoidal components of the load and the Active Power Filter are found, in the sinusoidal imposition of the regulator:

$$i^*_a=i^1_c a+i^1_f a$$

This remark results in the imposition of the Active Power Filter:

$$i_{ref}a=-k\tilde{i}=-k\left(\tilde{i}_f a(t)+\sum_k i_c a_k(t)+i_c a_q(t)\right)$$

proportional to the polluting component. If it is correctly designed in steady state, the controller cancels the steady state error:

$$\tilde{i}_f a(t)=-\left(\sum_k i_c a_k(t)+i_c a_q(t)\right)$$

so, the Active Power Filter will generate the polluting component itself necessary for the nonlinear load.

The assessment ε_{DC} from the regulator for charging capacitor C is converted to current reference, as follows:

$$\begin{cases} i^*_a=\varepsilon_{DC}\cdot\sin\omega t \\ i^*_b=\varepsilon_{DC}\cdot\sin\left(\omega t-2\pi/3\right) \\ i^*_c=\varepsilon_{DC}\cdot\sin\left(\omega t-4\pi/3\right) \end{cases}$$

Sinusoidal signal in phase with fundamental is obtained with Phase-Locked Loop (PLL), which allows the synchronization of the compensation signal and the voltage of the power supply system.

Fig. 4 presents the control diagram of the Active Power Filter using the Indirect Control method.

2.3.2 Synchronous Reference Frame (DQ)

This method obtains the reference currents starting from the nonlinear load currents where the compensation currents are not affected by disturbances and voltage imbalance at the source. This method converts the real currents into the synchronous reference frame (dq). This transformation is defined by Refs. [14, 15]:

$$\begin{bmatrix} i_d \\ i_q \end{bmatrix}=\begin{bmatrix} \cos(\omega t) & \sin(\omega t) \\ \sin(\omega t) & \cos(\omega t) \end{bmatrix}\cdot\begin{bmatrix} i_\alpha \\ i_\beta \end{bmatrix}$$

The terms d and q are composed of a DC component and a plurality of alternative components:

$$\begin{cases} i_d=i_{dcc}+i_{dac} \\ i_q=i_{qcc}+i_{qac} \end{cases}$$

The reference signs expressed in the real plan a-b-c:

$$\begin{bmatrix} i_{ref}a \\ i_{ref}b \\ i_{ref}c \end{bmatrix}=\sqrt{\frac{2}{3}}\cdot\begin{bmatrix} 1/\sqrt{2} & 1 & 0 \\ 1/\sqrt{2} & -1/2 & \sqrt{3}/2 \\ 1/\sqrt{2} & -1/2 & -\sqrt{3}/2 \end{bmatrix}\cdot\begin{bmatrix} -1 & 0 & 0 \\ 0 & \cos(\omega t) & -\sin(\omega t) \\ 0 & \sin(\omega t) & \cos(\omega t) \end{bmatrix}\cdot\begin{bmatrix} i_0 \\ i_{dref} \\ i_{qref} \end{bmatrix}$$

Fig. 5 presents the block diagram of the Active Power Filter control by the Synchronous Reference Frame (dq).

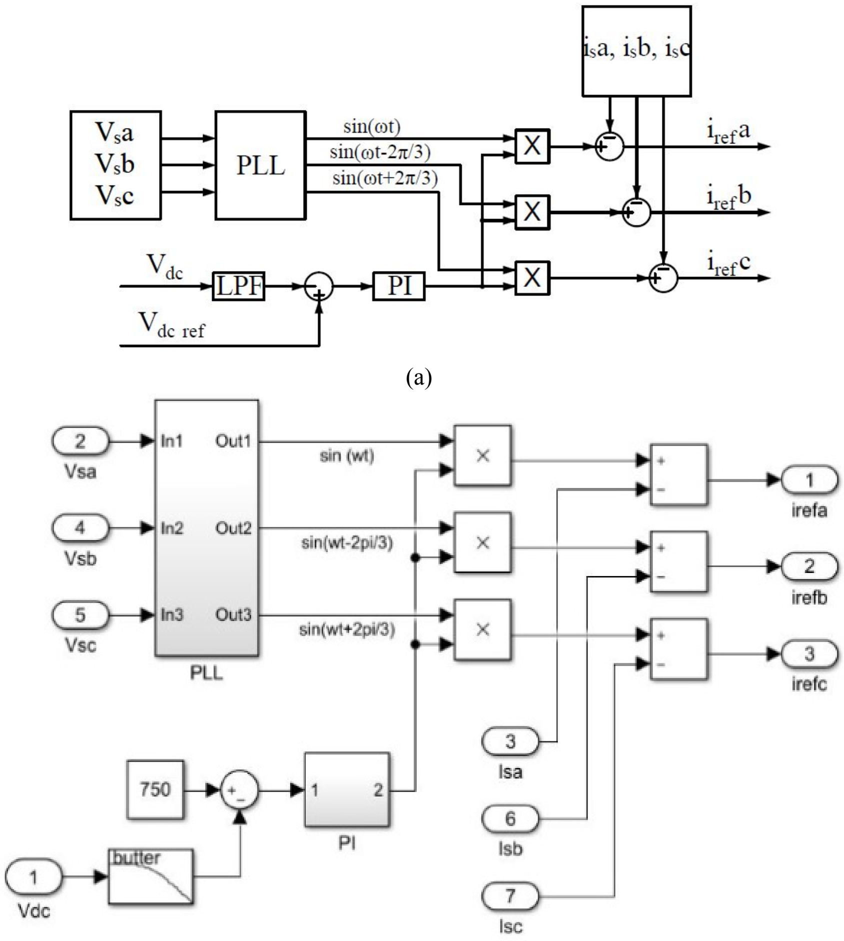

Fig. 4 Indirect control: (a) Block diagram; (b) Matlab/Simulink diagram.

2.3.3 Instantaneous Power (PQ)

This method is based on the transformation Clark of the reference system *abc* into the reference system *αβ* and the calculation of the instantaneous powers *p* and respectively *q*. Three-phase current and voltage are transformed into *αβ* coordinates using the equation [16, 17]:

$$\begin{bmatrix} V\alpha \\ V\beta \end{bmatrix} = \sqrt{\frac{2}{3}} \cdot \begin{bmatrix} 1 & -1/2 & -1/2 \\ 0 & \sqrt{3}/2 & -\sqrt{3}/2 \end{bmatrix} \cdot \begin{bmatrix} V_s a \\ V_s b \\ V_s c \end{bmatrix}$$

$$\begin{bmatrix} i\alpha \\ i\beta \end{bmatrix} = \sqrt{\frac{2}{3}} \cdot \begin{bmatrix} 1 & -1/2 & -1/2 \\ 0 & \sqrt{3}/2 & -\sqrt{3}/2 \end{bmatrix} \cdot \begin{bmatrix} i_c a \\ i_c b \\ i_c c \end{bmatrix}$$

After Clarke's transformation of current and voltage, it is followed by the instantaneous determination of power. Real power and reactive powers are calculated with:

$$\begin{bmatrix} p = \overline{p} + \tilde{p} \\ q = \overline{q} + \tilde{q} \end{bmatrix} = \begin{bmatrix} V\alpha & V\beta \\ -V\beta & V\alpha \end{bmatrix} \cdot \begin{bmatrix} i\alpha \\ i\beta \end{bmatrix}$$

The expression of currents as a function of instantaneous powers in the α-β plane is given by:

$$\begin{bmatrix} i\alpha \\ i\beta \end{bmatrix} = \frac{1}{V\alpha^2 + V\beta^2} \begin{bmatrix} V\alpha & V\beta \\ V\beta & V\alpha \end{bmatrix}^{-1} \cdot \begin{bmatrix} -\tilde{P} \\ -\tilde{Q} \end{bmatrix}$$

To calculate the reference signal, the harmonic currents in the tick system will be transformed by the Clarke inverse transformation:

$$\begin{bmatrix} i_{ref} a \\ i_{ref} b \\ i_{ref} c \end{bmatrix} = \sqrt{\frac{2}{3}} \begin{bmatrix} 1 & 0 \\ -1/2 & \sqrt{3}/2 \\ -1/2 & -\sqrt{3}/2 \end{bmatrix} \cdot \begin{bmatrix} i\alpha \\ i\beta \end{bmatrix}$$

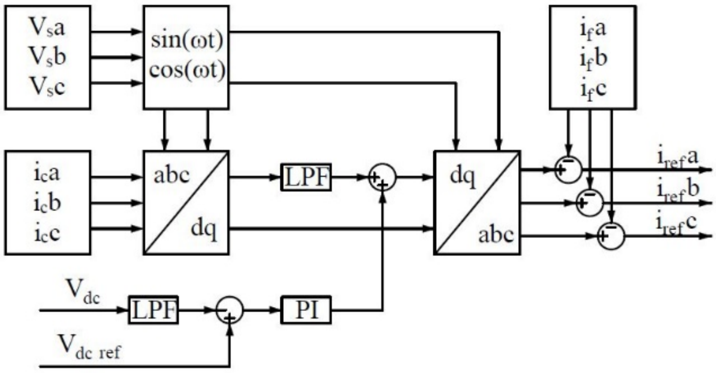

(a)

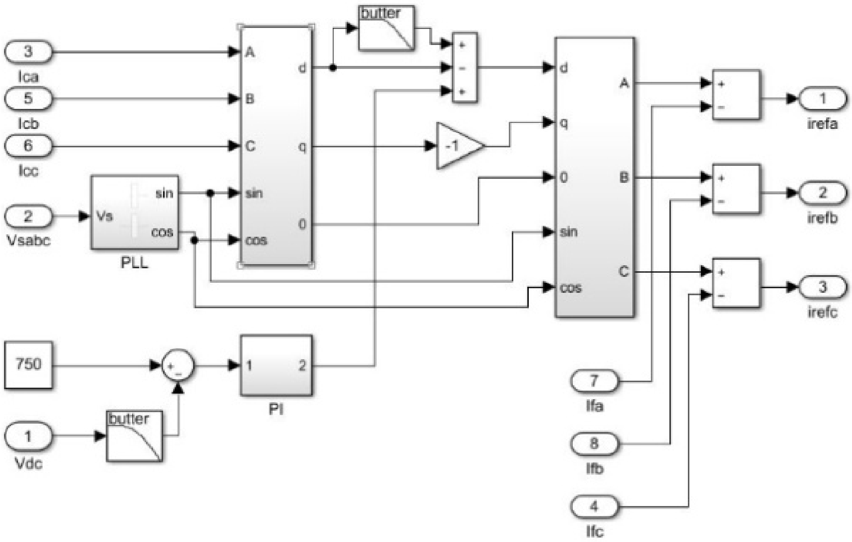

(b)

Fig. 5 Synchronous reference frame: (a) Block diagram; (b) Matlab/Simulink diagram.

Fig. 6 presents the block diagram of the Active Power Filter control by the Instantaneous power (PQ) method.

2.3.4 Positive Sequence Method (MSP)

This method works with the balanced current from the source, in phase with the positive sequence of the voltage from the source [18]:

$$\begin{bmatrix} i_{ref}a \\ i_{ref}b \\ i_{ref}c \end{bmatrix} = \begin{bmatrix} i_c a \\ i_c b \\ i_c c \end{bmatrix} - Ism \cdot \begin{bmatrix} \sin(\omega t + \mathrm{f}_f^+) \\ \sin(\omega t + \mathrm{f}_f^+ - 2\pi/3) \\ \sin(\omega t + \mathrm{f}_f^+ + 2\pi/3) \end{bmatrix}$$

where:

Ism—the magnitude of the current from the source;

f_f^+ —phase angle of the Fortescue transformation positive sequence fundamental components of the source voltages.

Extraction of *Ism:*

• Extraction of the fundamental component of the voltage from the source. We pass the source voltages through a low pass filter (LPF) and obtain the fundamental sinusoidal component;

• Extraction of the positive sequence of the fundamental component of the source voltage V_f^+.

$$[F] = \frac{1}{3} \cdot \begin{bmatrix} 1 & a & a^2 \\ 1 & a^2 & 1 \\ 1 & 1 & 1 \end{bmatrix}$$

The positive, negative and homopolar sequences are given by the relation:

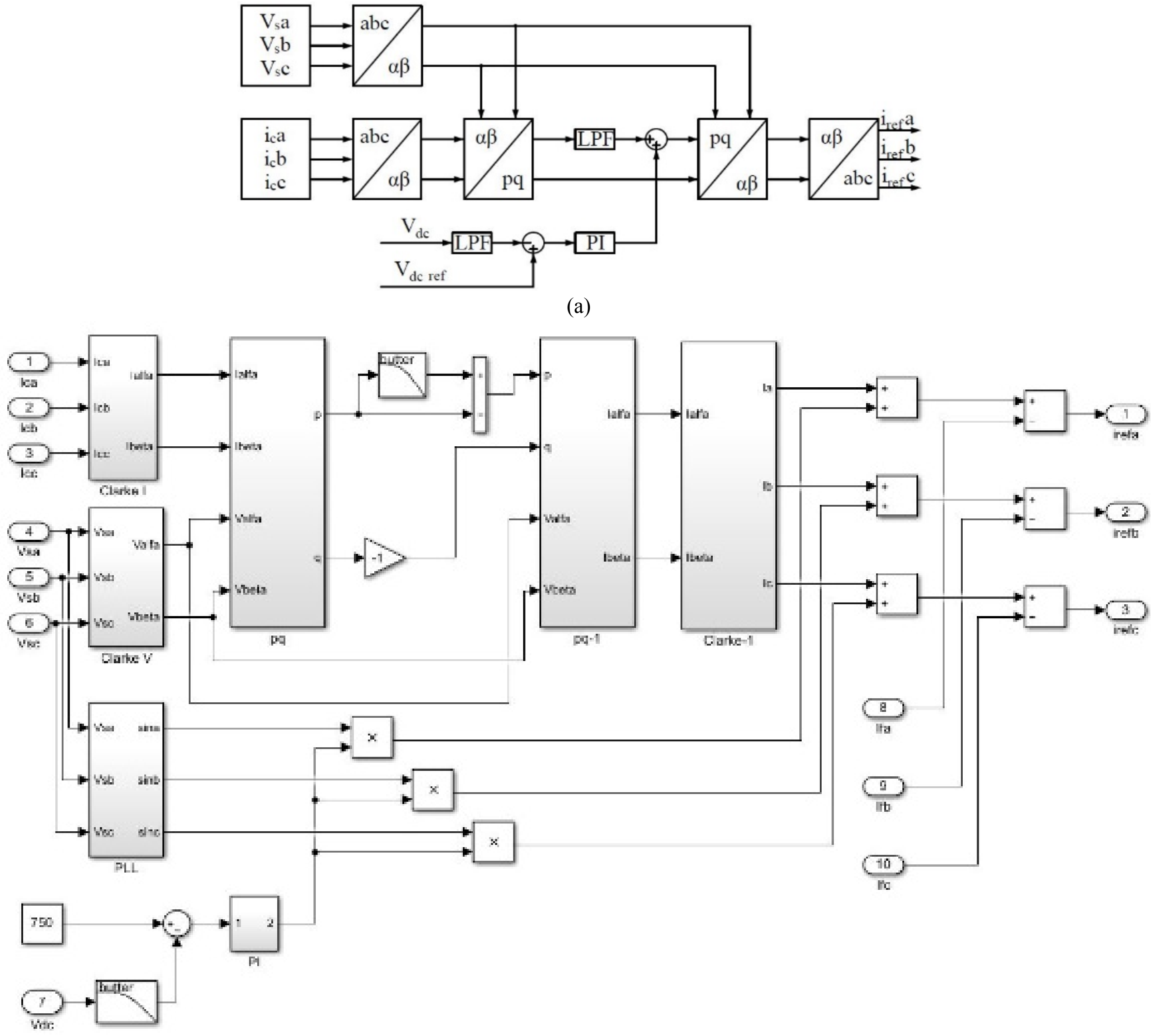

Fig. 6 Instantaneous power: (a) Block diagram; (b) Matlab/Simulink diagram.

$$\begin{bmatrix} \bar{V}_f^+ \\ \bar{V}_f^- \\ \bar{V}_f^0 \end{bmatrix} = [F] \cdot \begin{bmatrix} \bar{V}_{af} \\ \bar{V}_{bf} \\ \bar{V}_{cf} \end{bmatrix}$$

Active power P_c is the average value of instantaneous power p_c. We can deduce it from the equation below:

$$P_c = \frac{1}{T}\int_0^T p_c(t)dt$$

The active power of the source P_s is equal to the active power of the load P_c:

where:

$$\begin{cases} p_{sf}^+ = v_{af}^+ \cdot i_{sa} + v_{bf}^+ \cdot i_{sb} + v_{cf}^+ \cdot i_{sc} \\ p_{sf}^- = v_{af}^- \cdot i_{sa} + v_{bf}^- \cdot i_{sb} + v_{cf}^- \cdot i_{sc} \\ p_{sf}^0 = v_{af}^0 \cdot i_{sa} + v_{bf}^0 \cdot i_{sb} + v_{cf}^0 \cdot i_{sc} \\ p_{sh}^+ = \sum_{h=2}^{\infty} \left\{ v_{ah}^+ \cdot i_{sa} + v_{bh}^+ \cdot i_{sb} + v_{ch}^+ \cdot i_{sc} \right\} \\ p_{sh}^- = \sum_{h=2}^{\infty} \left\{ v_{ah}^- \cdot i_{sa} + v_{bh}^- \cdot i_{sb} + v_{ch}^- \cdot i_{sc} \right\} \\ p_{sh}^0 = \sum_{h=2}^{\infty} \left\{ v_{ah}^0 \cdot i_{sa} + v_{bh}^0 \cdot i_{sb} + v_{ch}^0 \cdot i_{sc} \right\} \end{cases}$$

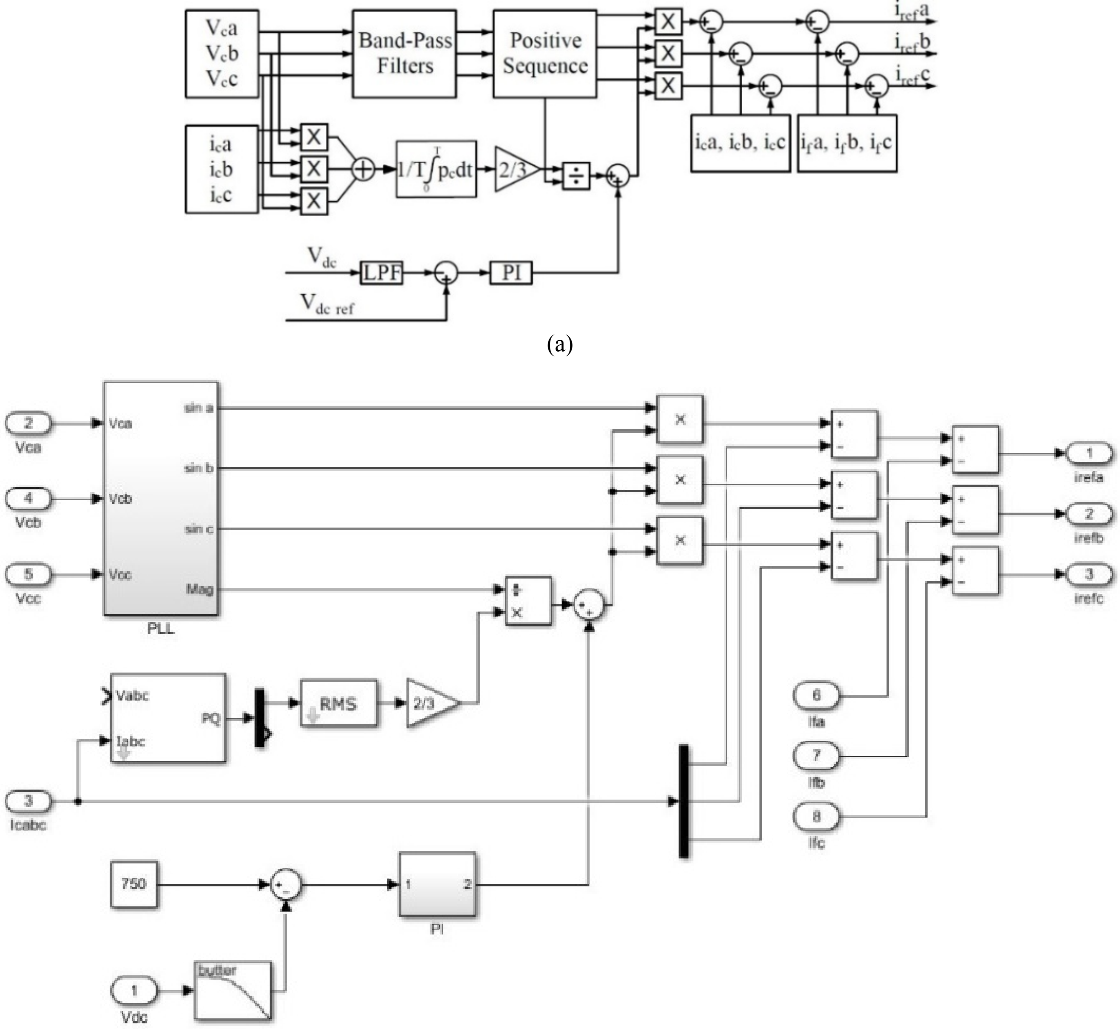

(a)

(b)

Fig. 7 Positive sequence method: (a) Block diagram; (b) Matlab/Simulink diagram.

And

$$\begin{bmatrix} v_{af}^{+} \\ v_{bf}^{+} \\ v_{cf}^{+} \end{bmatrix} = V_{mf}^{+} \cdot \begin{bmatrix} \sin\left(\omega t + \mathrm{f}_f^{+}\right) \\ \sin\left(\omega t + \mathrm{f}_f^{+} - 2\cdot\pi/3\right) \\ \sin\left(\omega t + \mathrm{f}_f^{+} + 2\cdot\pi/3\right) \end{bmatrix}$$

$$\begin{bmatrix} v_{af}^{-} \\ v_{bf}^{-} \\ v_{cf}^{-} \end{bmatrix} = V_{mf}^{-} \cdot \begin{bmatrix} \sin\left(\omega t + \mathrm{f}_f^{-}\right) \\ \sin\left(\omega t + \mathrm{f}_f^{-} - 2\cdot\pi/3\right) \\ \sin\left(\omega t + \mathrm{f}_f^{-} + 2\cdot\pi/3\right) \end{bmatrix}$$

$$v_{af}^{0} = v_{bf}^{0} = v_{cf}^{0} = V_{mf}^{0} \cdot \sin\left(\omega t + \mathrm{f}_f^{0}\right)$$

$$\begin{bmatrix} v_{ah}^{+} \\ v_{bh}^{+} \\ v_{ch}^{+} \end{bmatrix} = V_{mf}^{+} \cdot \begin{bmatrix} \sin\left(h\cdot\omega t + \mathrm{f}_f^{+}\right) \\ \sin\left(h\cdot\left(\omega t - 2\cdot\pi/3\right) + \mathrm{f}_f^{+}\right) \\ \sin\left(h\cdot\left(\omega t + 2\cdot\pi/3\right) + \mathrm{f}_f^{+}\right) \end{bmatrix}$$

$$\begin{bmatrix} v_{ah}^{-} \\ v_{bh}^{-} \\ v_{ch}^{-} \end{bmatrix} = V_{mf}^{-} \cdot \begin{bmatrix} \sin\left(h\cdot\omega t + \mathrm{f}_f^{-}\right) \\ \sin\left(h\cdot\left(\omega t - 2\cdot\pi/3\right) + \mathrm{f}_f^{-}\right) \\ \sin\left(h\cdot\left(\omega t + 2\cdot\pi/3\right) + \mathrm{f}_f^{-}\right) \end{bmatrix}$$

$$v_{ah}^{0} = v_{bh}^{0} = v_{ch}^{0} = V_{mh}^{0} \cdot \sin\left(h\cdot\omega t + \mathrm{f}_h^{0}\right)$$

Following the calculation, we obtain:

$$p_{sf}^{-} = p_{sf}^{0} = p_{sh}^{+} = p_{sh}^{-} = p_{sh}^{0} = 0$$

Resulting:

$$P_s = \frac{1}{T}\int_0^T p_{sf}^{+}(t)dt$$

Obtain:

$$P_c = P_s = 3/2 \cdot V_{mf}^{+} \cdot I_{sm}$$

which ultimately results in:

$$I_{sm} = \frac{2}{3} \cdot \frac{P_c}{V_{mf}^{+}}$$

Fig. 7 presents the block diagram of the Active Power Filter control by the Positive Sequence Method (MSP).

3. Results

In order to highlight the performances of this unitary system, simulations were performed in Matlab/Simulink in case of feeding the nonlinear load from the grid.

The results were presented in Figs. 8 and 9, where we can visualize a change in the sinusoidal form of the voltage and current.

Next, in order to be able to compare the presented control methods of the Active Power Filter, simulations were performed in Matlab/Simulink where the two distinct cases of the photovoltaic system were taken into account:

When the solar radiation is imposed at *I*r = 1,000 W/m^2, the photovoltaic system produces a power *P* = 7,300 W, which allows the supply of nonlinear charge and the excess power is injected into the grid;

In the other case when the solar radiation is imposed at *I*r = 250 W/m^2, the photovoltaic system produces a power of *P* = 1,780 W, which allows supplying the nonlinear load partially and the power difference is completed from the grid.

The power of the nonlinear load is set at *P* = 3,000 W.

3.1 Indirect Control (CI)

The voltage and current waveforms are presented in Fig. 10, where we can observe the sinusoidal forms of the voltage and the current from the grid.

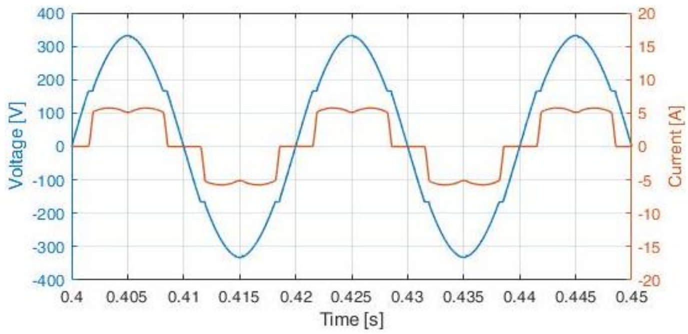

Fig. 8 Voltage and current waveforms.

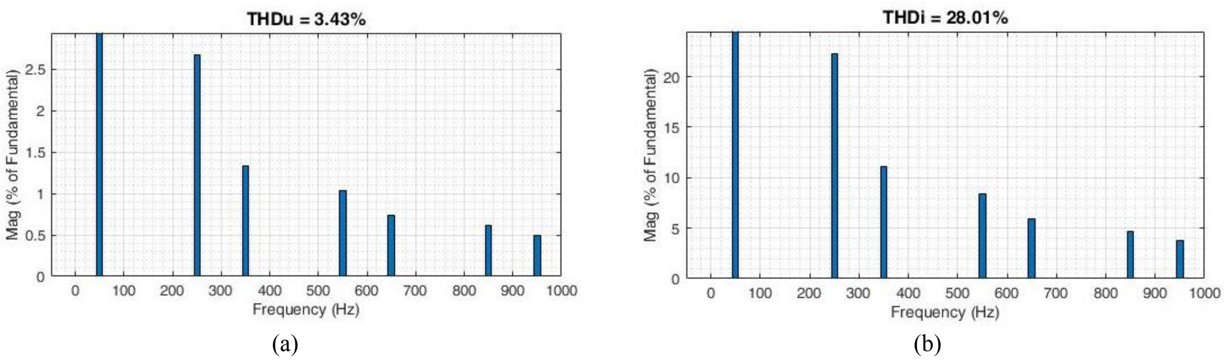

Fig. 9 The harmonic level of the nonlinear load: (a) Voltage; (b) current.

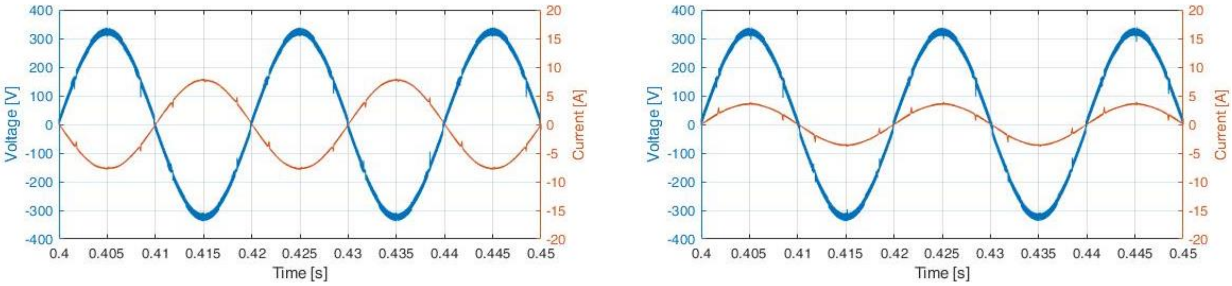

(a) (b)

Fig. 10 Grid voltage and current waveforms using the Indirect Control: (a) The photovoltaic system produces more power than the load; (b) The photovoltaic system produces less power than the load.

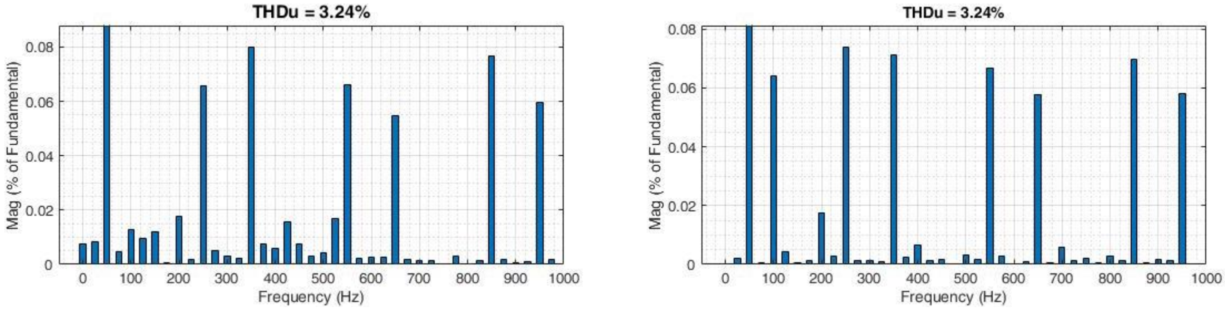

(a) (b)

Fig. 11 Harmonic level of grid voltage: (a) The photovoltaic system produces more power than the load; (b) The photovoltaic system produces less power than the load.

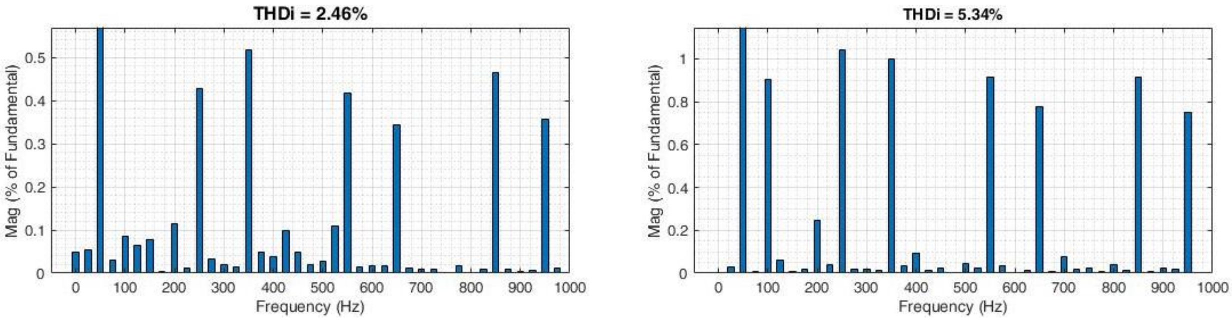

(a) (b)

Fig. 12 Harmonic level of grid current using the Indirect Control: (a) The photovoltaic system produces more power than the load; (b) The photovoltaic system produces less power than the load.

The determination of the total harmonic distortions of the grid voltage and current was performed using the Fast Fourier Transform (FFT). The results are present in Figs. 11 and 12.

3.2 Synchronous Reference Frame (DQ)

The voltage and current waveforms are presented in Fig. 13, where we can observe the sinusoidal forms of the voltage and the current from the grid.

The determination of the total harmonic distortions of the grid voltage and current was performed using the Fast Fourier Transform (FFT). The results were presented in Figs. 14 and 15.

3.3 Instantaneous Power (PQ)

The voltage and current waveforms are presented in Fig. 16, where we can observe the sinusoidal forms of the voltage and the current from the grid.

The determination of the total harmonic distortions of the grid voltage and current was performed using the Fast Fourier Transform (FFT). The results were presented in Figs. 17 and 18.

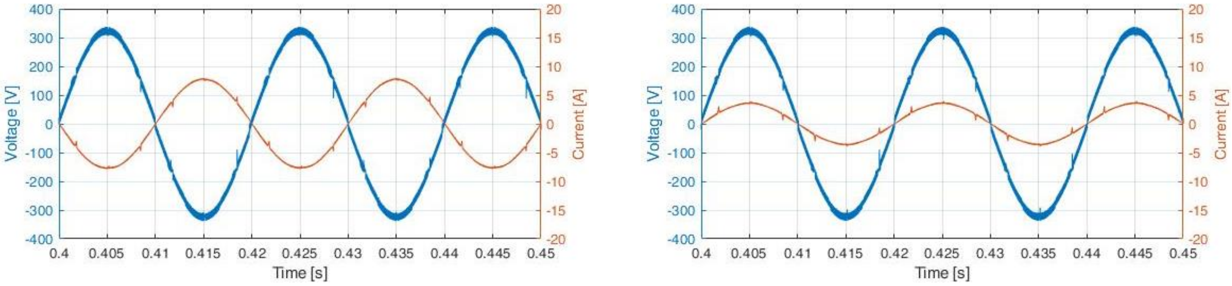

(a) (b)

Fig. 13 Grid voltage and current waveforms: (a) The photovoltaic system produces more power than the load; (b) The photovoltaic system produces less power than the load.

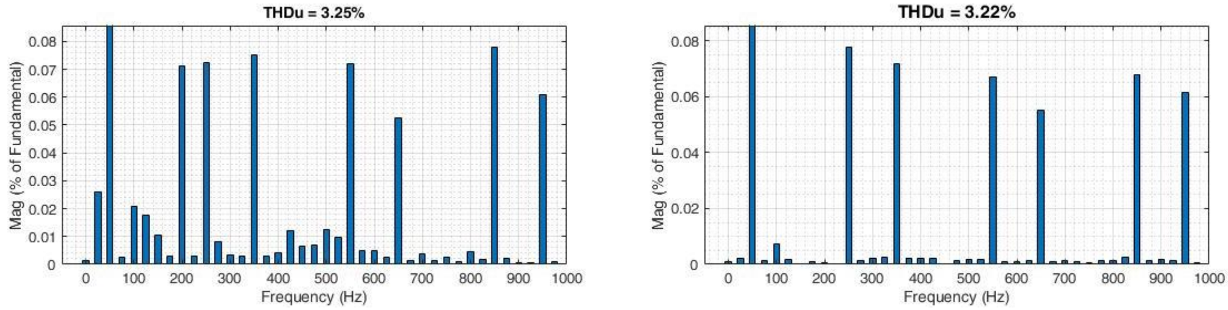

(a) (b)

Fig. 14 Harmonic level of grid voltage: (a) The photovoltaic system produces more power than the load; (b) The photovoltaic system produces less power than the load.

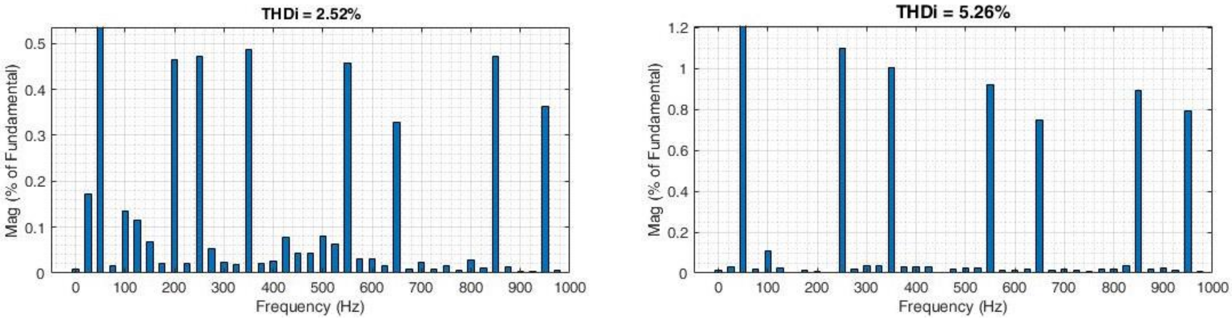

(a) (b)

Fig. 15 Harmonic level of grid current: (a) The photovoltaic system produces more power than the load; (b) The photovoltaic system produces less power than the load.

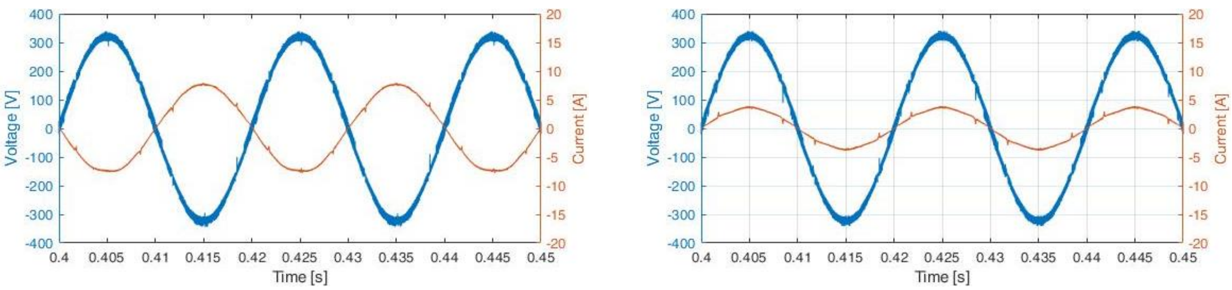

(a) (b)

Fig. 16 Grid voltage and current waveforms: (a) The photovoltaic system produces more power than the load; (b) The photo-voltaic system produces less power than the load.

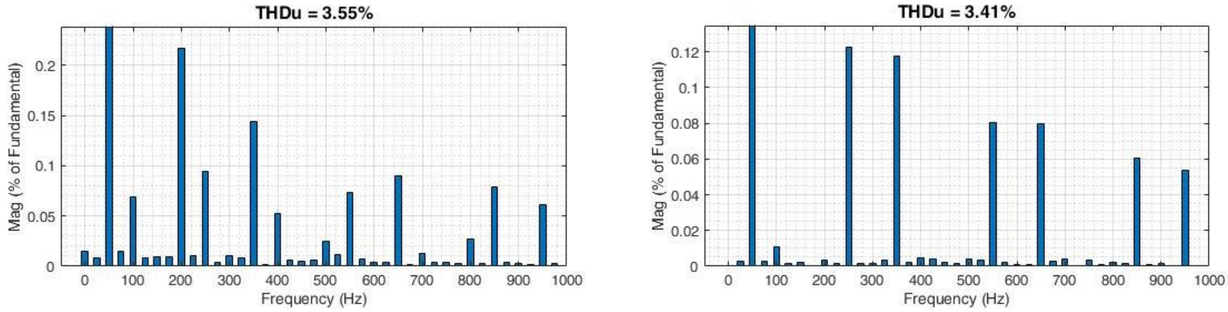

(a) (b)

Fig. 17 Harmonic level of grid voltage using the Instantaneous power: (a) The photovoltaic system produces more power than the load; (b) The photovoltaic system produces less power than the load.

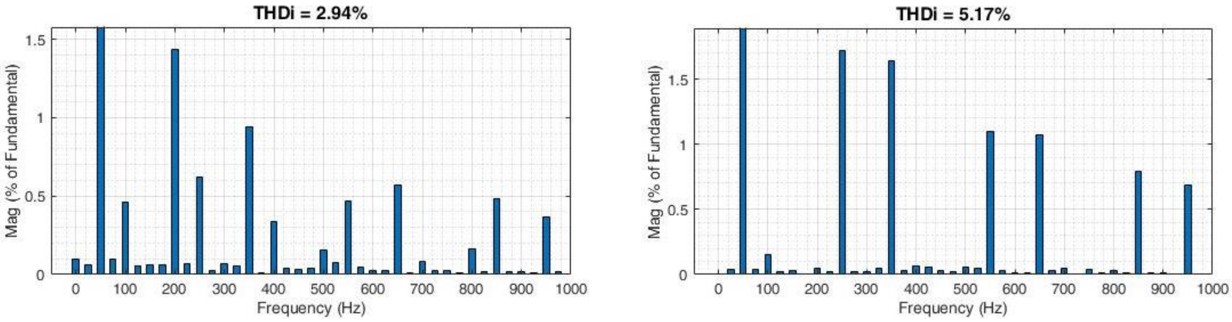

(a) (b)

Fig. 18 Harmonic level of grid current using the Instantaneous power: (a) The photovoltaic system produces more power than the load; (b) The photovoltaic system produces less power than the load.

3.4 Positive Sequence Method (MSP)

The voltage and current waveforms are presented in Fig. 19, where we can observe the sinusoidal forms of the voltage and the current from the grid.

The determination of the total harmonic distortions of the grid voltage and current was performed using the Fast Fourier Transform (FFT). The results were presented in Figs. 20 and 21.

Following the modeling and simulations performed, the results obtained are presented in numerical and graphical form in Fig. 22.

The values used to perform the Matlab/Simulink simulations are presented in Table 1.

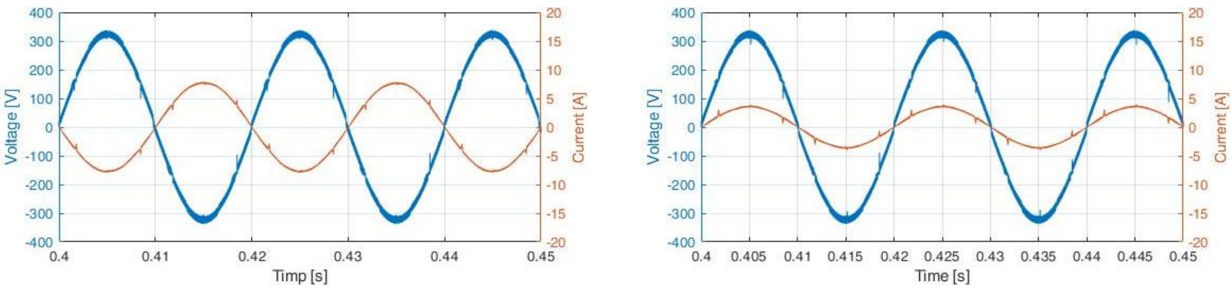

(a) (b)

Fig. 19 Grid voltage and current waveforms: (a) The photovoltaic system produces more power than the load; (b) The photo-voltaic system produces less power than the load.

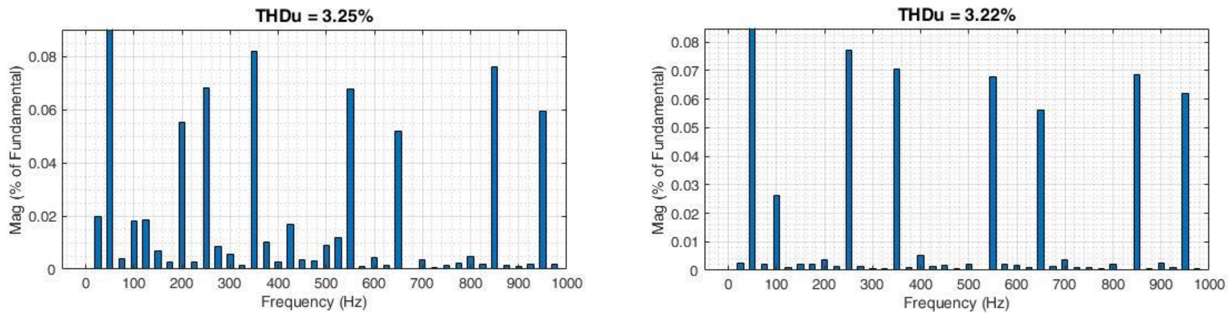

(a) (b)

Fig. 20 Harmonic level of grid voltage: (a) The photovoltaic system produces more power than the load; (b) The photovoltaic system produces less power than the load.

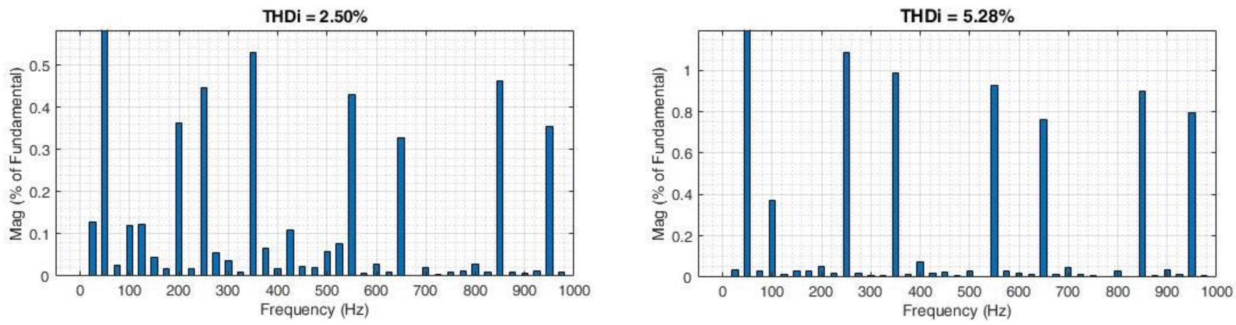

(a) (b)

Fig. 21 Harmonic level of grid current: (a) The photovoltaic system produces more power than the load; (b) The photovoltaic system produces less power than the load.

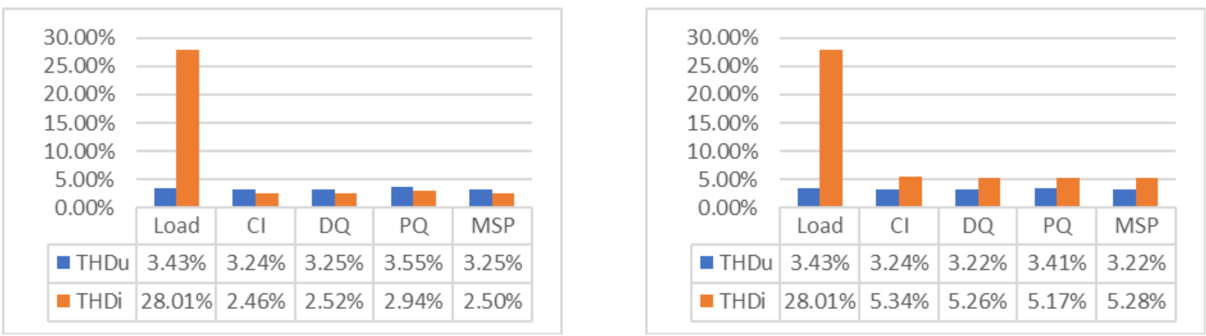

(a) (b)

Fig. 22 Comparative analysis of the harmonic level of grid voltage and current and nonlinear load: (a) The photovoltaic system produces more power than the load; (b) The photovoltaic system produces less power than the load.

Table 1 Values used to simulate.

Equipment	Date	Value	Unit
Grid	Line voltage (U_L)	400	V
	Apparent power (S)	25,000	VA
Nonlinear load	Resistance (R)	97	Ω
Boost converter	Inductance (L)	0.0045	H
	Capacitance (C)	2.65×10^{-5}	F
	Switching frequency IGBT (F_{sw})	25,000	Hz
Photovoltaic panel (LG365Q1C-A5)	Peak Power (P_{max})	365	W
	Open-circuit Voltage (V_{oc})	42.8	V
	Voltage at P_{max} (V_{mp})	36.7	V
	Short-circuit current (I_{sc})	10.8	A

Table 1 to be continued

	Current at P_{max} (I_{mp})	9.95	A
	Series/Parallel	10/2	Panels
	Temperature (T)	25	°C
Active power filter	Inductance (L)	0.0055	H
	Capacitance (C)	0.001	F
	Switching frequency IGBT (F_{sw})	25,000	Hz
	Continuous voltage of the APF (V_{dc})	750	V
Proportional and integral (PI) controllers	The proportional coefficient (kp)	1	
	The integral coefficient (ki)	20	

4. Conclusions

In this paper, the results were compared in the case of injecting renewable energy from the photovoltaic system to the grid through the Active Power Filter where 4 control methods were used.

The Matlab/Simulink simulations demonstrated the performance of this system which allows at the same time the interconnection of the photovoltaic system to the grid and the improvement of electricity quality.

Following the results obtained we can see that the use of any of the control methods allows the injection of energy into the grid produced by the photovoltaic system and improve the quality of electricity.

Analyzing the results in detail, it can be stated that the Indirect Control (CI) method obtains THDu = 3.24%, THDi = 2.46% with the best results if the photovoltaic system produces a power greater than the nonlinear load and the excess is injected into the grid.

In the other case when the photovoltaic system produces a power less than the non-linear load and the difference is completed by the grid. Synchronous Reference Frame (DQ) THDu = 3.22%, THDi = 5.26% and Instantaneous power (PQ) THDu = 3.41%, THDi = 5.17% methods get the best results.

Acknowledgment

This study was supported by the CRESC INTEL project "Knowledge Transfer Regarding the Energy Efficiency Increase and Intelligent Power Systems", ID/Cod My SMIS: P_40_340/105803, project co-funded by the European Union from the European Regional Development Fund through the Competitiveness Operational Program 2014-2020.

References

[1] Sriranjani, R., and Jayalalitha, S. 2018. "PV Interconnected Shunt Active Filter for Power Balancing and Harmonic." *Pure and Applied Mathematics* 118: 2341-54.

[2] Vaquero, J., Vázquez, N., Soriano, I., and Vázquez, J. 2018. "Grid-Connected Photovoltaic System with Active Power Filtering Functionality." *Photoenergy* 2018: 1-9.

[3] Bouzelata, Y., Kurt, E., Altin, N., and Chenni, R. 2015. "Design and Simulation of a Solar Supplied Multifunctional Active Power Filter and a Comparative Study on the Current-Detection Algorithms." *Renewable and Sustainable Energy Reviews* 43: 1114-26.

[4] Kannan, V. K., and Rengarajan, N. 2013. "Control of Photovoltaic System with A DC-DC Boost Converter Fed DSTATCOM Using IcosΦ Algorithm." *Applied and Engineering* 16: 89-98.

[5] Djeghader, Y., Chelli, Z., and Rehaimia, S. 2018. "Harmonic Mitigation in Electrical Grid Connected Renewable Energy Sources." *ACTA Electrotehnica* 59: 287-91.

[6] Vijayakumar, M., and Vijayan, S. 2014. "Design and Implementation of PV-Based Three-Phase Four-Wire Series Hybrid Active Power Filter for Power Quality Improvement." *Sādhanā* 39: 859-77.

[7] Hadpe, N. V., Tapre, P. C., and Solanki, A. M. 2019. "Design and Performance Analysis of Three-Phase Solar PV Integrated UPQC." *IRJET* 6: 6426-30.

[8] Bouzelata, Y., Kurt, E., Chenni, R., and Necmi, A. 2015. "Design and Simulation of a Unified Power Quality Conditioner Fed by Solar Energy." *Hydrogen Energy* 40: 15267-77.

[9] Muthuvel, K., and Vijayakumar, M. 2020. "Solar PV Sustained Quasi Z-Source Network-Based Unified Power Quality Conditioner for Enhancement of Power Quality." *Energies* 13: 1-26.

[10] Livinti, P., and Ghandour, M. 2020. "Fuzzy Logic System for Controlling of DC/DC Boost Converter Developed in

MATLAB SIMULINK." *IRJET* 7: 1-8.

[11] Dusa, A. 2020. "Integration of Photovoltaic Systems in a Low Voltage Electrical Grid." *The Annals of "Dunărea de Jos" University of Galati* 43: 28-35.

[12] Kamran, M., Mudassar, M., Fazal, M. R., Asghar, M. U., Bilal, M., and Asghar, R. 2020. "Implementation of Improved Perturb & Observe MPPT Technique with Confined Search Space for Standalone Photovoltaic System." *King Saud University Engineering Sciences* 32: 432-41.

[13] Gurguiatu, G., and Munteanu, T. 2012. "Indirect Control in Active Power Filters." In *Proceedings of the 13th International Conference on Optimization of Electrical and Electronic Equipment*, Brasov, Romania.

[14] Dusa, A., Balanuta, C. D., Gurguiatu, G., and Niculcea, A. N. 2019. "Reactive Power Compensation for a PV Park Connected at a Long Distance." In *Proceedings of the 6th International Symposium on Electrical and Electronics Engineering*, Galati, Romania, October 18-20, 2019.

[15] Balanuta, C. D., Dusa, A., Gurguiatu, G., and Luca, L. 2019. "Reactive Power Compensation for Consumers Connected at Long-Distances." In *Proceedings of the 6th International Symposium on Electrical and Electronics Engineering, Galati*, Romania, October 18-20, 2019.

[16] Suhendar Firmansyah, T., Maulana, A., and Zuldiag Vektor, D. 2017. "Shunt Active Power Filter Based on P-Q Theory with Multilevel Inverters for Harmonic Current Compensation." *Telkomnika* 15: 1632-40.

[17] Watanabe, E. H., Aredes, M., and Akagi, H. 2004. "The P-Q Theory for Active Filter Control: Some Problems and Solutions." *Controle & Automação* 15: 78-84.

[18] Benalla, H., and Djeghloud, H. 2006. "A Novel Time-Domain Reference-Computation Algorithm for Shunt Active Power Filters." *ACSE* 6: 33-40.